IJCRT.ORG ISSN : 2320-2882

INTERNATIONAL JOURNAL OF CREATIVE RESEARCH THOUGHTS (IJCRT)

An International Open Access, Peer-reviewed, Refereed Journal

Second Order Sliding Mode Control of DSIG Connected to the Grid

Housseyn KAHAL*, Abdelkader BOUYEKNI, Rachid TALEB, Zinelaabidine BOUDJEMA

Electrical Engineering Department, Hassiba Benbouali University, Chlef, Algeria
Laboratoire Génie Electrique et Energies Renouvelables (LGEER)

Abstract: Multiphase asynchronous machines are used more and more for reasons of reliability and power segmentation. This study deals with the modeling and the control of a dual star induction generator (DSIG) connected to the grid via two rectifiers and a three-phase inverter controlled by PWM. A second order sliding mode has been applied to the DSIG control. The last part of this work was devoted to the integration of the DSIG in the wind energy conversion system. The results of simulations presented at the end of this work show the effectiveness of the proposed control in particular on the quality of the energy supplied to the grid.

Index Terms **- Dual star induction generator (DSIG), second order sliding mode control (SOSMC), field oriented control (FOC), PWM rectifier.**

I. INTRODUCTION

In the last years, wind energy as the most widely utilized renewable resources and has been installed all over the world [1]. The reason is that the energy it produces does not cause greenhouse gases or other pollutants. Modern wind turbines use advanced power electronics to provide efficient generator control and to ensure compatible operation with the power system [2].

There are many wind generator technologies, among which the dual stator induction generator (DSIG). The DSIG has a stator winding more than the ordinary induction generator [3, 4]; they are spatially shifted by 30 electrical degrees with isolated neutral points. Thus the state equations become more complicated as well as the coupling among the state variables. This paper concentrates on the mathematical model of DSIG whose stator windings are tight coupled. A simplified DSIG model is given as well.

In the past years the control strategy of a variable-structure using the sliding mode control (SMC) has been the subject of many studies and researches for machine control [5], The sliding mode control system advantage is that the controller is switched between two various control structures [6].

Though, this kind of control has an essential flaw, which is the chattering phenomen on produced by the discontinuous control action. To fix these difficulties, several Amendments to the original SMC law have been suggested, the most important being the boundary layer approach [7].

One manner to enhance SMC performance is to use a second order sliding mode controller [8].

This paper is structured as follows. Modeling of the dual star induction and the vector control strategy (Fields and voltages equations is given) are shown in Section 2. The field oriented control (FOC) of a DSIG is presented in Section 3. The Second Order Sliding Mode Control (SOSMC) are developed in Section 4. The integration of the DSIG in the wind energy conversion system in Section 5.The scheme presented in Figure 3.1 and 4.3 are used for numerical simulation and the associated results are presented. Finally, the conclusions of this work are drawn.

II. MATHEMATICAL MODEL OF DSIG

The representation of the DSIG in the graduation Park is given in the following equivalent schemes.

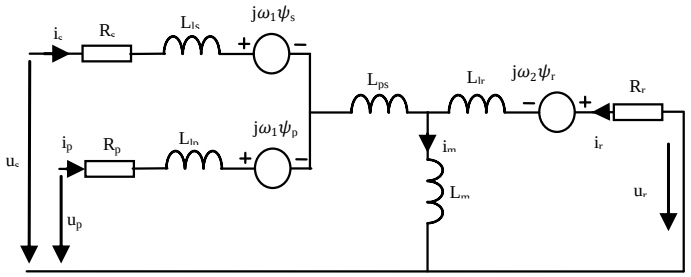

Figure 2.1: The d-q equivalent circuit of the DSIG

2.1The voltages equations

The expressions of the stator and rotor voltage are defined by the following equation system:

$$\begin{cases} v_{ds1} = -R_{s1}i_{ds1} + \frac{d}{dt}\emptyset_{ds1} - \omega_s\emptyset_{qs1} \\ v_{qs1} = -R_{s1}i_{qs1} + \frac{d}{dt}\emptyset_{qs1} + \omega_s\emptyset_{ds1} \\ v_{ds2} = -R_{s2}i_{ds2} + \frac{d}{dt}\emptyset_{ds2} - \omega_s\emptyset_{qs2} \\ v_{qs2} = -R_{s2}i_{qs2} + \frac{d}{dt}\emptyset_{qs2} + \omega_s\emptyset_{ds2} \\ 0 = R_r i_{dr} + \frac{d}{dt}\emptyset_{dr} - (\omega_s - \omega_r)\emptyset_{qr} \\ 0 = R_r i_{qr} + \frac{d}{dt}\emptyset_{qr} + (\omega_s - \omega_r)\emptyset_{dr} \end{cases} \quad (2.1)$$

2.2 The flux equations

The expressions of the stator and rotor flux are defined by the following equation system:

$$\begin{cases} \emptyset_{ds1} = -l_{s1}i_{ds1} - l_m(i_{ds1} + i_{ds2}) + L_{md}(-i_{ds1} - i_{ds2} + i_{dr}) - L_{dq}\,i_{qs2} \\ \emptyset_{qs1} = -l_{s1}i_{qs1} - l_m(i_{qs1} + i_{qs2}) + L_{mq}(-i_{qs1} - i_{qs2} + i_{qr}) + L_{dq}\,i_{ds2} \\ \emptyset_{ds2} = -l_{s2}i_{ds2} - l_m(i_{ds1} + i_{ds2}) + L_{md}(-i_{ds1} - i_{ds2} + i_{dr}) + L_{dq}\,i_{qs1} \\ \emptyset_{qs2} = -l_{s2}i_{qs2} - l_m(i_{qs1} + i_{qs2}) + L_{mq}(-i_{qs1} - i_{qs2} + i_{qr}) - L_{dq}\,i_{ds1} \\ \emptyset_{dr} = l_r i_{dr} + L_{md}(-i_{ds1} - i_{ds2} + i_{dr}) \\ \emptyset_{qr} = l_r i_{qr} + L_{mq}(-i_{qs1} - i_{qs2} + i_{qr}) \end{cases} \quad (2.2)$$

2.3 Electromagnetic torque

The expression of electromagnetic torque of the DSIG is written:

$$T_{em} = \left(\frac{3}{2}\right)\left(\frac{p}{2}\right)\left(\frac{L_m}{L_{dr}}\right)[(i_{qs1} + i_{qs2})]\emptyset_{dr} - (i_{ds1} + i_{ds2})\emptyset_{qr} \quad (2.3)$$

III. CONTROL STRATEGY OF THE SYSTEM

3.1 The control rotor field orientation

In this control strategy, the field vector coincides with d-q axis. Then the component ϕ_{qr} is zero and ϕ_{dr} is constant. The advantage of this presentation is to have à constant size in permanent regime.

$$\begin{aligned} \emptyset_{dr} &= \emptyset_r^* \\ \emptyset_{qr} &= 0 \\ p\emptyset_r^* &= 0 \end{aligned} \quad (3.1)$$

The application of the rotor field orientation on the model of the DSIG given by the voltages equations:

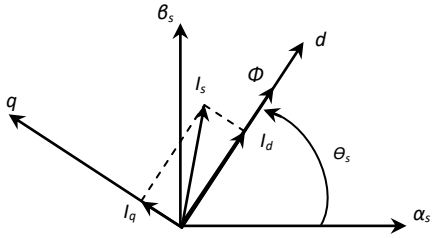

Figure 3.1: Fundament of Rotor Field Orientation.

We obtain:

$$\begin{cases} i_{dr} = 0 \\ i_{qr} = -\frac{(\omega_s - \omega_r)\emptyset_r^*}{R_r} \end{cases} \quad (3.2)$$

The final torque expression is written:

$$T_{em}^{*} = \left(\frac{3}{2}\right)\left(\frac{p}{2}\right)\frac{L_m}{L_m+L_r}\left(i_{qs1}+i_{qs2}\right)\emptyset_r^{*} \qquad (3.3)$$

3.2 The Control algorithm

The objective of our control is to maintain constant the voltage at the output of the two rectifiers. The expression of the reference power is written:

$$V_{dc}\, i_{dc} = P^{*} = P_{ele} = T_{em}\,\Omega \qquad (3.4)$$

The torque expression is:

$$T_{em} = \frac{P^{*}}{\Omega} \qquad (3.5)$$

The torque is controlled by the quadrature of current iqs1 and i_{qs2} of the two stators:

$$i_{qs1} + i_{qs2} = \frac{(L_m+L_r)T_{em}^{*}}{p\,L_m\,\emptyset_r^{*}} \qquad (3.6)$$

The flux ϕ_r* is estimated from the currents isd1 and i_{sd2} of the two stators:

$$\emptyset_r^{*} = \frac{R_r L_m}{(L_r+L_m)P+R_r}\left(i_{ds1}+i_{ds2}\right) \qquad (3.7)$$

3.3 Sliding mode controller (SMC)

To avoid chattering some approaches were proposed. The main idea was to change the dynamics in small vicinity of the discontinuity surface in order to avoid real discontinuity and at the same time to preserve the main properties of the whole system.

$$\dot{x} = f(x,t) + B(x,t)V(x,t), x \in R^{n}, V \in R^{m}, ran\left(B(x,t)\right) = m \qquad (3.8)$$

With control in the sliding mode, the goal is to keep the system motion on the manifold S [7], which is defined as:

$$S = \{x : e(x,t) = 0\} \qquad (3.9)$$

And

$$e = x^{*} - x \qquad (3.10)$$

With
e : is the tracking error vector,
x* is the desired state,
x is the state vector.

The sliding mode control should be chosen such that the candidate Lyapunov function satisfies the Lyapunov stability criteria:

$$\vartheta = \frac{1}{2}S(x)^2 \qquad (3.11)$$

$$\dot{\vartheta} = S(x)\dot{S}(x) \qquad (3.12)$$

This can be assured for:

$$\dot{\vartheta} = -\eta|S(x)| \qquad (3.13)$$

With η>0.

Essentially, equation (3.11) states that the squared "distance" to the surface, measured by $e(x)^2$, decreases along all system trajectories. Therefore (3.12), (3.13) satisfy the Lyapunov condition. With selected Lyapunov function the stability of the whole control system is guaranteed. The control function will satisfy reaching conditions in the following form:

$$U^{com} = U^{eq} + U^{n} \qquad (3.14)$$

With :
U^{com} is the control vector.
U^{eq} is the equivalent control vector.
U^{n} is the correction factor and must be calculated so that the stability conditions for the selected control are satisfied.

$$U^{n} = K sat(S(x)/\delta) \qquad (3.15)$$

sat((S(x)/δ) is the proposed saturation function, δ is the boundary layer thickness. In this paper we propose the Slotine method [9]:

$$S(X) = \left(\frac{d}{dt}+\lambda\right)^{n-1} e \qquad (3.16)$$

Here, *e* is the tracking error vector, λ is a positive coefficient and *n* is the relative degree.
In our study, we choose the error between the measured and reference voltage of the DSIG as sliding mode surface, so we can write the following expression:

$$S = V^*_{dc} - V_{dc} \qquad (3.17)$$

The first order derivate, gives :

$$\dot{S} = \dot{V}^*_{dc} - \dot{V}_{dc} \qquad (3.18)$$

The sliding mode will exist only if the following condition is met:

$$\dot{S}.S < 0 \qquad (3.19)$$

3.4 Second order sliding mode controller (SOSMC)

This method generalizes the essential sliding mode idea by acting on the higher order time derivatives of the sliding manifold, instead of influencing the first time derivative as it is the case in SMC, therefore reducing chattering and avoiding strong mechanical efforts while preserving SMC advantages.

In order to ensure the DSIG voltage convergence to their reference, a second order sliding mode control (SOSMC) is used. Considering the sliding mode surface given by (3.18), the following expression can be written:

$$\begin{cases} \dot{S} = \dot{V}^*_{dc} - \dot{V}_{dc} \\ \ddot{S} = Y(t,x) + \Lambda(t,x) I_{Rq} \end{cases} \qquad (3.20)$$

Where Y(t,x) and Λ(t,x) are uncertain functions which satisfy:

$$Y > 0, |Y| > \lambda, 0 < K_m < \Lambda < K_M \qquad (3.21)$$

Basing on the super twisting algorithm introduced by Levant in [10], the proposed high order sliding mode controller contains two parts:

$$I_{Rq} = v_1 + v_2 \qquad (3.22)$$

With

$$\dot{v}_1 = -k.sign(S)$$
$$v_2 = -l.|S|^{\gamma}.sign(S)$$

In order to ensure the convergence of the sliding manifolds to zero in finite time, the gains can be chosen as follows [11].

$$\begin{cases} k > \frac{\lambda}{K_m} \\ l^2 \geq \frac{4\lambda}{K_m^2} \frac{K_M(k+\lambda)}{K_m(k-\lambda)} \\ 0 < \gamma \leq 0.5 \end{cases} \qquad (3.23)$$

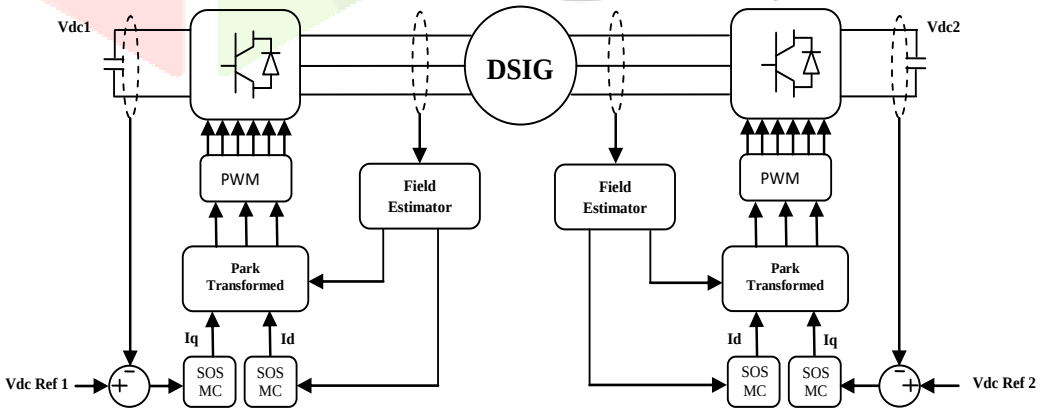

Figure 3.1: Block diagram of the DSIG voltage control with SOSMC

IV. CONTROL OF THE DSIG CONNECTED TO THE GRID

The studied system is connected to the grid, considered powerful and consists of a wind generator based on a DSIG, three power converters, DC bus and transformer. The overall diagram of the system is shown in figure 4.1.

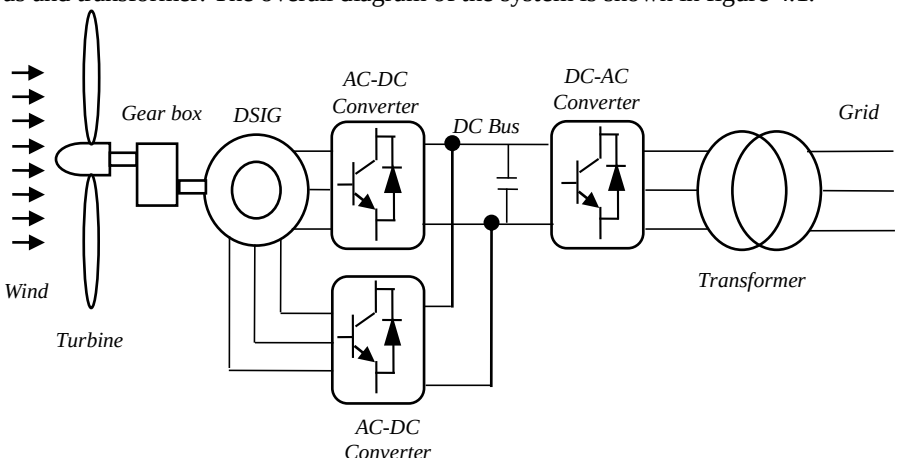

Figure 4.1: Schematic representation of the DSIG connected to the grid.

4.1. Modeling of the grid side inverter

The line voltages are:

$$\begin{cases} V_{AB} = V_{as} - V_{bs} = E \cdot (f_1 + f_2) \\ V_{BC} = V_{bs} - V_{cs} = E \cdot (f_2 + f_3) \\ V_{CA} = V_{cs} - V_{as} = E \cdot (f_3 + f_1) \end{cases} \quad (4.1)$$

With

$f_i + \bar{f}_i = 1 \ \ avec \ \ i = 1,2,3$

The phase-to-neutral voltages V_{as1}, V_{as2} and V_{as3} form a balanced three-phase system, such as:

$$V_{as1} + V_{bs1} + V_{cs1} = 0 \quad (4.2)$$

Solving equations (4.1) and (4.2) gives us:

$$\begin{bmatrix} V_{as} \\ V_{bs} \\ V_{cs} \end{bmatrix} = \frac{E}{2} \begin{bmatrix} 2 & -1 & -1 \\ -1 & 2 & -1 \\ -1 & -1 & 2 \end{bmatrix} \begin{bmatrix} f_1 \\ f_2 \\ f_3 \end{bmatrix} \quad (4.3)$$

4.2. Calculation of DC bus voltage

The voltage of the DC bus (V_{dc}) is linked to the effective phase-to-neutral voltage of the grid (V_{eff}) by the relation (4.4):

$$V_{dc} = \gamma V_{eff} 2\sqrt{2} \quad (4.4)$$

Where γ is the dimensioning parameter of the DC bus, which in our case is taken equal to 1.
After calculations, we find: V_{dc} = 1130 V.

4.3. Electric grid modeling

The power grid model is shown in Figure 4.2.

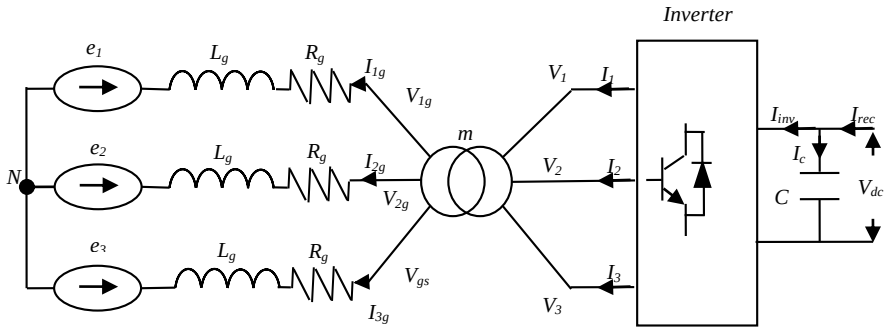

Figure 4.2: Electric grid model.

The analytical model of the grid is presented by the system of equations (4.5), where e_1, e_2 and e_3 present the electromotive force of the grid; R_g and L_g are respectively the resistance and the inductance of the lines.

$$\begin{cases} V_{1g} - e_1 = R_g \cdot I_{1g} + L_g \cdot \frac{dI_{1g}}{dt} \\ V_{2g} - e_2 = R_g \cdot I_{2g} + L_g \cdot \frac{dI_{2g}}{dt} \\ V_{3g} - e_3 = R_g \cdot I_{3g} + L_g \cdot \frac{dI_{3g}}{dt} \end{cases} \quad (4.5)$$

The expressions for the active and reactive powers injected into the grid are given by equation (4.6).

$$\begin{aligned} P_g &= V_{dg} i_{dg} + V_{qg} i_{qg} \\ Q_g &= V_{qg} i_{dg} - V_{dg} i_{qg} \end{aligned} \quad (4.6)$$

4.4. Grid link control

The block diagram representation of the principle of the control of the connection to the grid is illustrated by figure 4.3.

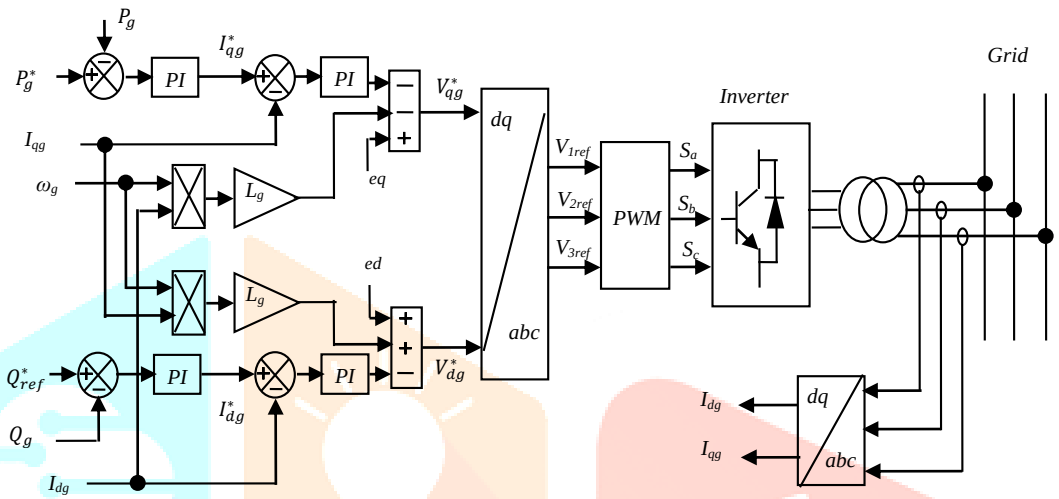

Figure 4.3: Schematic representation of the principle of the control of the connection to the grid.

From the desired active and reactive powers, the converter is controlled so as to impose references to the phase-to-neutral voltages (V_{dg}, V_{qg}). The Park components of the currents (I_{dg}, I_{qg}) are regulated by *PI* correctors with compensation, such as:

$$\begin{aligned} V_{dg}^* &= V_{rd}^* + e_d - \omega_g L_g I_{qg} \\ V_{qg}^* &= V_{rq}^* + e_q + \omega_g L_g I_{dg} \end{aligned} \quad (4.7)$$

With :

$$\begin{aligned} V_{rd}^* &= PI\left(I_{dg}^* - i_{dg}\right) \\ V_{rq}^* &= PI\left(I_{qg}^* - i_{qg}\right) \end{aligned} \quad (4.8)$$

The reference active power is estimated by (4.9), where η_1 and η_2 is the efficiency of the mechanical conversion.

$$P_g^* = P_1 + P_2 = \eta_1 \frac{1}{2} C_{P1}(\lambda,\beta) \rho \pi R_1^2 V_1^3 + \eta_2 \frac{1}{2} C_{P2}(\lambda,\beta) \rho \pi R_2^2 V_2^3 \quad (4.9)$$

The active power is adjusted by a regulation loop based on a *PI* corrector generating the current reference (I^*_{qg}).

$$I_{qg}^* = PI\left(P_g^* - P_g\right) \quad (4.10)$$

The adjustment of the reactive power is carried out in the same way as with the active power.

$$I_{dg}^* = PI\left(Q_g^* - Q_g\right) \quad (4.11)$$

V. SIMULATION RESULTS AND DISCUSSIONS

In this session, we will present the simulation results of the wind power conversion chain, based on DSIG. The simulation is performed by the Matlab / Simulink software (the Grid and DSIG parameters are given in Table 1, 2). The reference active power (P_g^*) injected into the grid is limited to the value of 1.5 MW (i.e. the nominal power of the DSIG used) and the reference reactive power is set at a zero value $Q_g^* = 0$ to have a unit power factor.

The wind profile is chosen randomly (Figure 5.1).

Figure 5.2 represents the mechanical speed of the DSIG and its reference. We can see that the mechanical speed Ω_{mec} is controlled and perfectly follows its reference.

The two components of the rotor field of the DSIG according to the two direct and quadratic axes are given by figures 5.3 and 5.4. The direct rotor field component (ϕ_{dr}) follows its reference and the quadratic rotor field component (ϕ_{qr}) is zero. This is due to the directional control of the rotor field, carried out in conjunction with the SOSMC.

The evolution of the DC bus voltage is given by figure 5.5, where the reference voltage is equal to 1130 V. Note that the voltage V_{dc} is kept constant and follows its reference perfectly, while exhibiting variations around the latter of negligible magnitude.

The shape of the voltage at the output of the first phase PWM inverter during the limited power operation zone is shown in Figure 5.6.

The current flow on the grid side of the first phase is given in figure 5.7. The amplitude of the current injected into the grid is imposed by the technique of monitoring the connection to the grid. Their evolution during the full simulation time (zones II and III) is shown in figure 5.7 (A). During the limited power operation zone is shown in Figure 5.7(B).

Figure 5.8 represents the evolution of active and reactive power on the grid side. The active power injected into the grid changes in the same way as for the mechanical power.

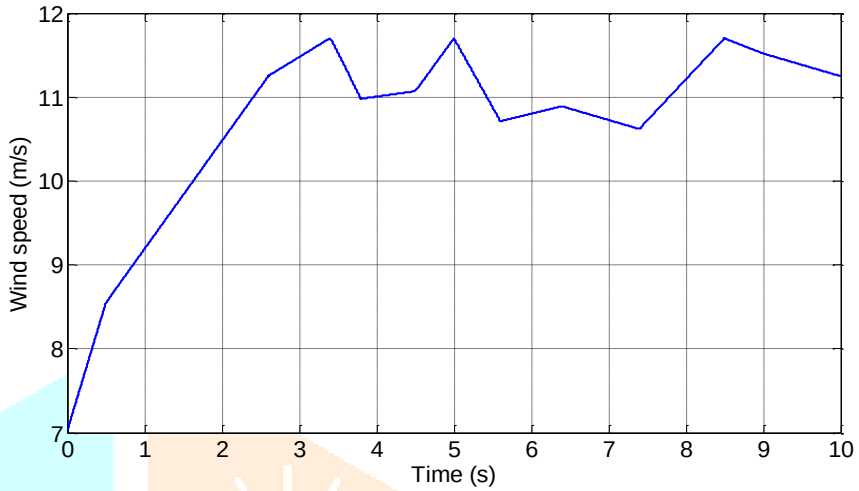

Figure 5.1: Wind profile

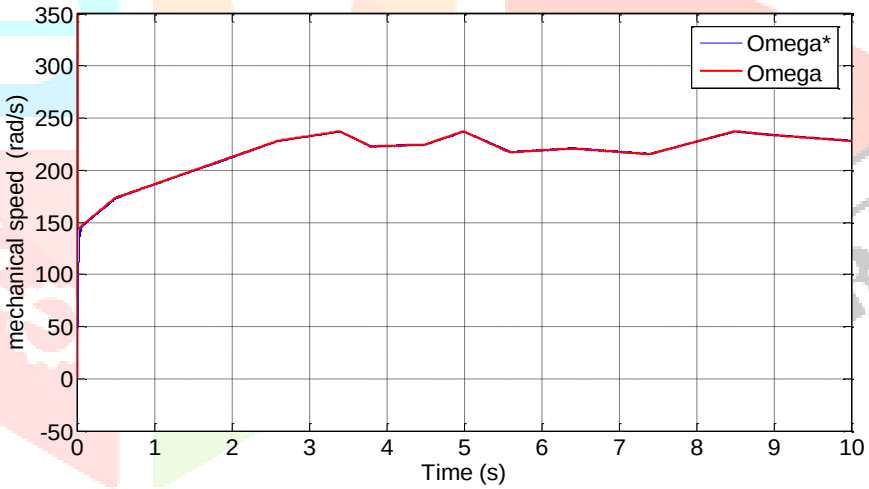

Figure 5.2: DSIG mechanical speed and its reference.

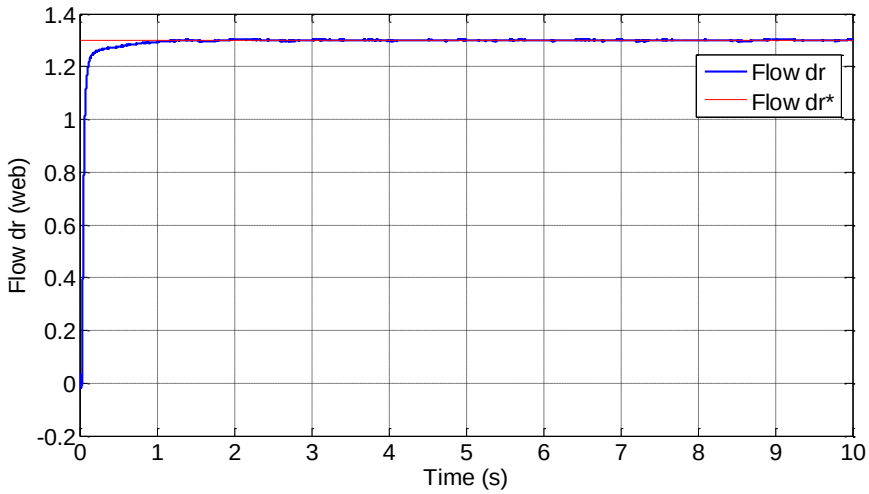

Figure 5.3: Direct rotor field and its reference

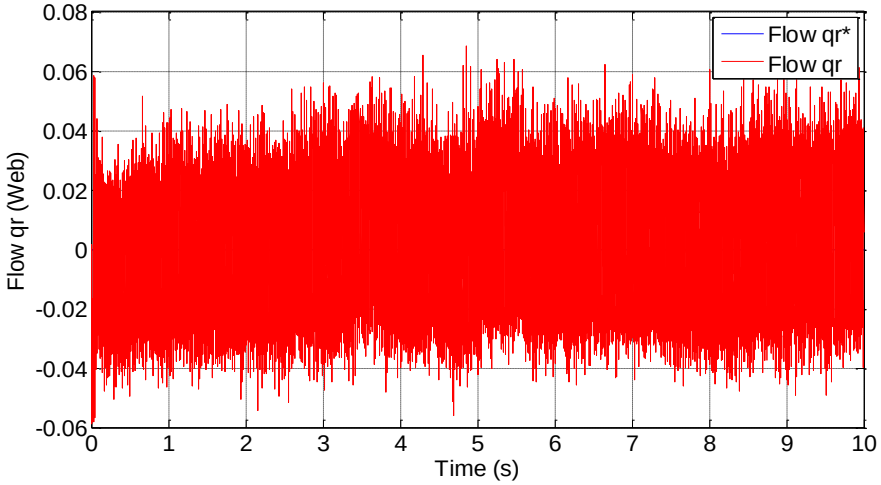

Figure 5.4: Rotor field in quadrature and its reference.

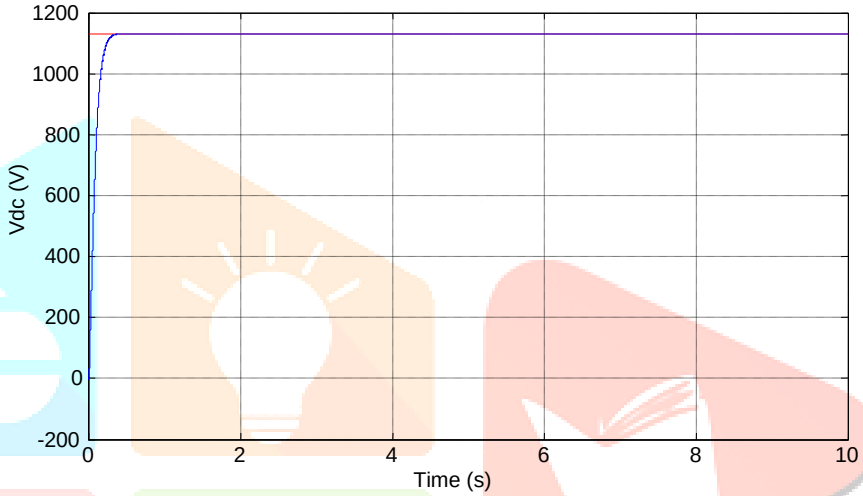

Figure 5.5: DC bus voltage

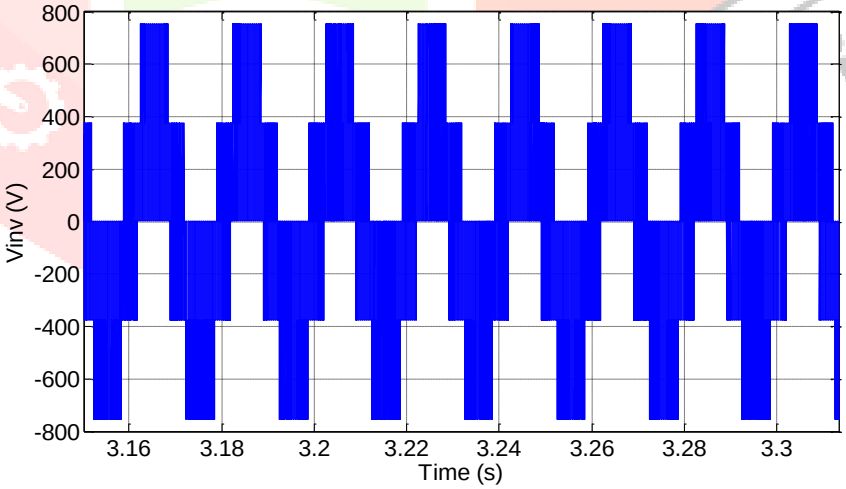

Figure 5.6: Voltage on inverter side

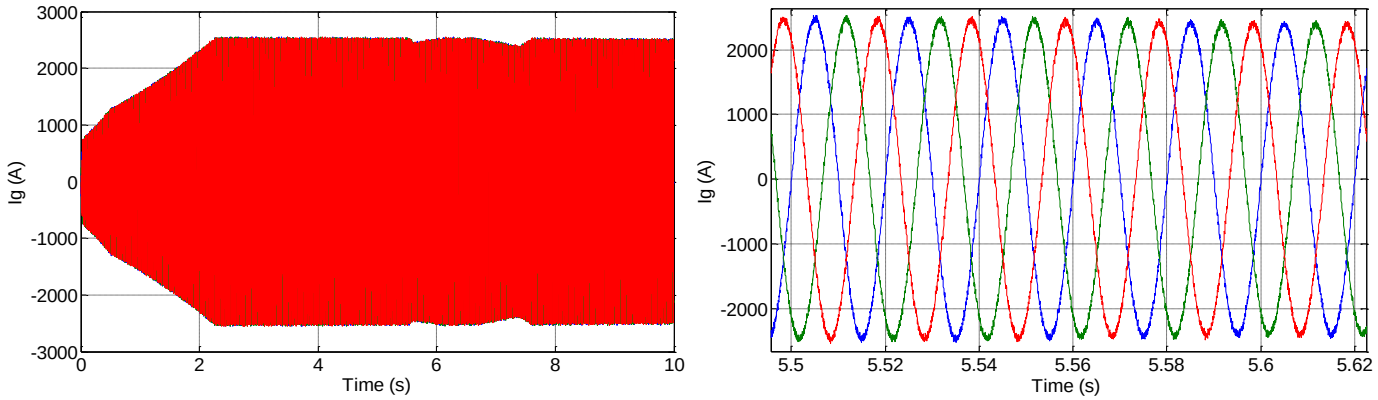

(A) Ig Current (B) Zoom on Ig current

Figure 5.7: Current on the grid side

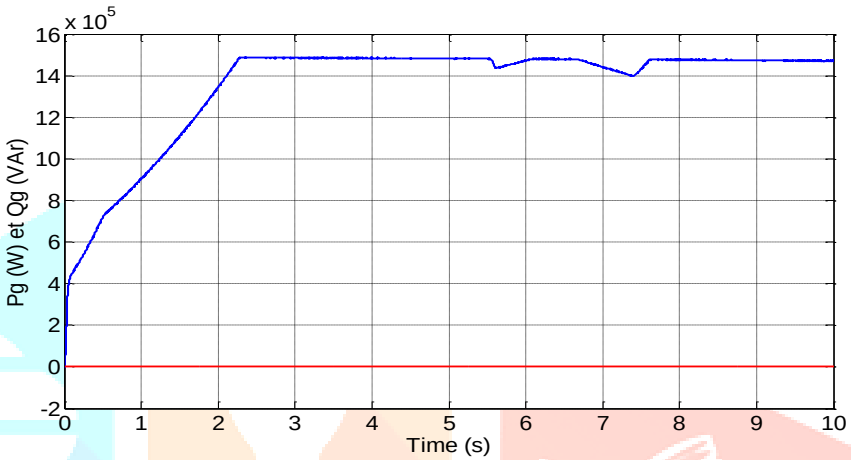

Figure 5.9: Grid side active and reactive power.

VI. CONCLUSIONS

The work presented in this paper generally concerns the study, modeling, control and simulation of a wind power system connected to the grid. We used the high order sliding mode control (SOSMC) technique. The control used was applied to control the voltages of the DC buses of the DSIG and satisfactory simulation results were obtained (speed and robustness).

In the second part of this work, we have dealt with the connection of the studied system to the electrical grid. This connection was ensured by PI type regulators and numerical simulation results were presented and discussed.

Table 1 The Grid and DC bus parameters

Parameters	Value	IS-Unit
DC bus voltage	1130	V
DC bus capacity	9.8	mF
Grid resistance	0.015	Ω
Grid inductance	0.002	H

Table 2 The DSIG parameters

Parameters	Value	IS-Unit
Stator voltage	400	V
Stator/rotor frequency	50	Hz
Stator 1 resistance	0.008	Ω
Stator 2 resistance	0.008	Ω
Rotor resistance	0.007	Ω
Stator 1 inductance	0.134	H
Stator 2 inductance	0.134	H
Rotor inductance	0.067	H
Mutual inductance	0.0045	H
Inertia	30	Kg.m2

VII. ACKNOWLEDGMENT

This work was financially supported by the the Electrical Engineering Department. Universty Hassiba Benbouali, Chlef, Algeria.

The data collection and theory in this paper are completed by the help of Mr. R Taleb, sam Department and university, to whom we express our heart feelings.

REFERENCES

[1] Bendjeddou, Y .2013. Contribution à l'étude des performances d'un générateur asynchrone, Master Thesis, Hadj Lakhdar Uninversity, Batna.

[2] Anaya-Lara, O. Jenkins, N. Ekanayake, J. Cartwright, P and Hughes, M. 2009. Wind Energy Generation: Modelling and Control, John Wiley & Sons, Ltd.

[3] Hassan Zamani, M. Hossein Riahy, G and Abedi, M. 2016. Rotor-Speed Stability Improvement of Dual Stator-Winding Induction Generator-Based Wind Farms By Control-Windings Voltage Oriented Control. IEEE Transactions on Power Electronics, 31(8): 5538-5546.

[4] Liu, L. Li, J and Lu, C. 2009. Research on the real-time simulation system of dual stator winding induction generator with variable speed. 9th International Conference on Electronic Measurement & Instruments, Beijing, 3: 452-455.

[5] Martinez, M, I. Tapia, G. Susperregui, A. and Camblong, H. 2012. Sliding-Mode Control for DFIG Rotor- and Grid-Side Converters Under Unbalanced and Harmonically Distorted Grid Voltage. IEEE Transactions on Energy Conversion, 27(2): 328-339.

[6] Laamyad, T. Naceri, F. Abdessemed, R and Belkacem, S. 2013. A fuzzy sliding mode strategy for control of the dual star induction machine. Journal of Electrical Engineering, 13(1): 216-224.

[7] Sun, T. Chen, Z and Blaabjerg, F. 2005. Flicker study on variable speed wind turbines with doubly fed induction generators. IEEE Transactions on Energy Conversion, 20(4): 896-905.

[8] Boudjema, Z. Taleb, R. Yahdou, A. Kahal, H. 2015. High order sliding mode control of a DFIM supplied by two power inverters. Carpathian Journal of Electronic and Computer Engineering, 8(1): 23-30.

[9] Slotine, J J. Weiping, L. 1991. Applied Nonlinear Control. Prentice Hall, Englewood Cliffs, New Jersey 07632.

[10] Levant, A. 2003. Higher-order sliding modes, differentiation and output feedback control. International Journal of Control, 76(9-10): 924-941.

[11] Boudjema, Z. Taleb, R. Yahdou, A. Kahal, H. 2015. High order sliding mode control of a DFIM supplied by two power inverters. Carpathian Journal of Electronic and Computer Engineering, 8(1): 23-30.